scientific reports

Check for updates

OPEN

^{166}Dy/^{166}Ho-labeled porous hydroxyapatite microparticles for treatment of inflammatory joint diseases – Exploring the advantages of in vivo generator

Sourav Patra[1,2], Khajan Singh[1], Avik Chakraborty[2,3], Shahiralam Khan Mohammed[1], Sutapa Rakshit[2,3], Rubel Chakravarty[1,2] & Sudipta Chakraborty[1,2]✉

Holmium-166 [$T_{½}$ = 26.8 h, $E_{β}^{-}$ (max) = 1.74 MeV (48.7%) and 1.85 MeV (50.0%); Eγ = 80.6 keV (10.6%)] is one of the most promising radionuclides in radiation synovectomy (RSV) for the treatment of inflammatory joint diseases, especially of large joints. However, short half-life of ^{166}Ho is a practical impediment toward its extensive utility. This study aims to address this limitation by developing a potent formulation where ^{166}Ho in transient radioactive equilibrium with ^{166}Dy [$T_{½}$ = 81.5 h] is used as its in vivo generator. In this regard, a chelator-free radiolabeling approach was optimized using porous hydroxyapatite (HA) microsphere (2–10 µm) as a carrier platform of ^{166}Dy/^{166}Ho. Sorption of ^{166}Dy/^{166}Ho in porous HA followed Langmuir-Freundlich isotherm and pseudo-second order kinetics, indicating chemisorption of the radiolabeling process. The formulation retained its radiochemical integrity in PBS and human serum upto a period of 14 d. The preclinical study showed near-exclusive retention of the radiolabeled microparticles within the injected joint cavity of healthy Wistar rats with no translocation of ^{166}Dy and ^{166}Ho. Overall, the reported studies indicated the potency developed ^{166}Dy/^{166}Ho-labeled porous HA microsphere for the treatment of inflammatory joint diseases and an in vivo generator of ^{166}Ho.

Keywords Radiation synovectomy, ^{166}Dy/^{166}Ho equilibrium mixture, In vivo generator, Porous hydroxyapatite, Sorption capacity

Radiation synovectomy (RSV) involves intra-articular administration of $β^-$ emitting radionuclides after conjugating with microparticles of appropriate size (2–10 µm) and is an effective treatment modality for the patients suffering from chronic inflammatory joint diseases[1–8] In this therapeutic modality, radioactive microparticles are locally administered into the joint cavity and phagocytosed by the synovial macrophages in the diseased joint. Subsequently, the ionizing $β^-$ radiation ablates the proliferating cells of the inner layer of the synovium. In this process, the pain and effusion of the joint is reduced significantly for ~ 70% of the patients undergone the procedure[9] Despite these excellent attributes, the major disadvantage of RSV is associated with radiation exposer of heathy organs mainly liver and spleen due to leakage of radioactivity from the joint and its subsequent accumulation in the healthy organs as mentioned[10,11] The leakage could be attributed either to the small size of the radiolabled particulates or poor in vivo stability of the formulation that often leads to the disintegration of radioisotope from the particulate matrix[12] In this regard, hydroxyapatite (HA) microparticles of appropriate size (2–10 µm) is one of the most preferred carrier matrix due to its inherent biocompatibility and high affinity towards various therapeutic radioisotope with suitable decay properties, resulting in a robust radiolabeled formulation having excellent stability in *in* vivo[13–18] One such radioisotope is ^{166}Ho, which decays to stable ^{166}Er by $β^-$ emission followed by de-excitation by γ photon emission [$T_{½}$ = 26.8 h, $E_{β}^{-}$(max) = 1.74 MeV (48.7%) and 1.85 MeV (50.0%), Eγ = 80.6 keV (10.6%)][19–22]. The $β^-$ particles from the decay of ^{166}Ho results maximum soft tissue penetration depth 8.7 mm, although 90% of the total radiation dose is deposited within

[1]Radiopharmaceuticals Division, Bhabha Atomic Research Centre, Mumbai 400085, India. [2]Homi Bhabha National Institute, Anushaktinagar, Mumbai 400094, India. [3]Radiation Medicine Centre (Medical), Bhabha Atomic Research Centre, Mumbai 400012, India. ✉email: sudipta@barc.gov.in; sudiptac1273@gmail.com

the first 2.1 mm[23] Thus, ^{166}Ho could be considered as a potential candidate for the application of RSV for large joints[20–22].

Holmium-166 could be produced by two routes in nuclear reactor. The conventional direct route of production involves thermal neutron activation of ^{165}Ho by irradiation of natural Ho_2O_3 in nuclear reactor [natural abundance of ^{165}Ho is 100% and σ = 64 b for ^{165}Ho (n, γ)^{166}Ho][24] Apart from this, ^{166}Ho could also be produced by the indirect route which involves irradiation of Dy_2O_3 target in nuclear reactor. In this case, thermal neutron activation of ^{164}Dy (natural abundance 28.2%, σ = 2650 b) results in the production of ^{165}Dy [$T_{1/2}$ = 2.3 h, E_β^-(max) = 1.3 MeV (83%), Eγ = 94.8 keV (3.6%)] which on subsequent neutron capture produces ^{166}Dy [$T_{1/2}$ = 81.5 h, E_β^-(max) = 500 keV, Eγ = 82.7 (13%), 371.7 (0.46%) and 426.0 keV (0.54%), σ = 3600 b for ^{165}Dy(n, γ)^{166}Dy] that decays to ^{166}Ho by β^-emission[25,26]. Thereby, thermal neutron irradiation of Dy_2O_3 target in nuclear reactor would result in the production of an equilibrium mixture of ^{166}Dy (longer lived parent, $T_{1/2}$ = 81.5 h) and ^{166}Ho (shorter lived daughter, $T_{1/2}$ = 26.8 h).

The use of ^{166}Dy/^{166}Ho equilibrium mixture in RSV instead of ^{166}Ho produced from direct production route would prolong the irradiation of the diseased joint with the β^- emission from ^{166}Ho following the half-life of ^{166}Dy ($T_{1/2}$ = 81.5 h). Thus, this system would function as an in vivo generator of ^{166}Ho[27,28] Owing to its relatively short half-life, use of ^{166}Ho produced from direct route leads to practical impediment from supply logistic point of view. This could be overcome by using in vivo generator of ^{166}Ho in the form of the ^{166}Dy/^{166}Ho equilibrium mixture. Moreover, the Monte Carlo theoretical depth dose profiles in a joint model demonstrated that in RSV treatment with equal therapeutic dose to the synovium surface, in vivo generator system of ^{166}Dy/^{166}Ho would produce 50% and 25% less radiation dose to the bone surface and articular cartilage than that of pure ^{166}Ho[28] However, the major challenge associated with the use of ^{166}Dy/^{166}Ho equilibrium couple is the probable release of ^{166}Ho from the radiolabeled particulate. It has been reported that the chelation of ^{166}Dy/^{166}Ho with DOTA chelator released 72% of ^{166}Ho[29] This happens because ^{166}Dy decays to the excited state of ^{166}Ho by β^- emission. Subsequently, during the de-excitation of ^{166}Ho, a series of Augur electrons (~ 31 electron per decay) are ejected along with prompt γ photons. These Augur electrons are responsible for the destruction of DOTA complex and release of 72% of ^{166}Ho[29] Therefore, ^{166}Dy/^{166}Ho could be used as a potential in vivo generator only when the carrier platform precludes the loss of internally converted ^{166}Ho.

In the present work, we aimed at developing a robust radiolabeled formulation which could be utilized as an in vivo generator of ^{166}Ho, in which ^{166}Ho follows 81.5 h half-life of its parent ^{166}Dy, without compromising the radiochemical integrity of formulation. Working toward this, we have reported the production of ^{166}Ho by thermal neutron irradiation of Dy_2O_3 target and chelator–free radiolabeling of porous HA microsphere with the equilibrium mixture of ^{166}Dy/^{166}Ho. The utility of porous HA particles with high surface area was felt essential as it would facilitate formulation of stable radiolabeled product with anticipated low specific activity of ^{166}Ho (activity per unit mass of Dy target irradiated) in the ^{166}Dy/^{166}Ho mixture. The radiolabeling parameters were optimized and the sorption of ^{166}Dy/^{166}Ho on the surface of HA was investigated. The in vitro stability of the radiolabeled microparticle formulation was determined in phosphate buffer saline (PBS) and human serum. The pharmacokinetics of formulation was demonstrated by acquiring SPECT images and performing ex vivo biodistribution after intra-articular administration of ^{166}Dy/^{166}Ho-labeled HA in ankle joint of healthy Wistar rat. The possible translocation of ^{166}Ho from the instilled formulation in vivo was also investigated. The schematic representation of the work reported herein is given in Fig. 1.

Experimental

Materials and methods

Natural Dy_2O_3 (spectroscopic grade, > 99.99% chemically pure, 28.2% ^{164}Dy) powder was procured from American Potash Inc., USA. All other chemicals used in this study were AR grade and procured from Merck, India. Porous hydroxyapatite (HA) microparticles were synthesized by following the procedure reported by us earlier[1] Briefly, 50 mL of 1 M of calcium nitrate solution was added dropwise into 50 mL of 0.6 M potassium dihydrogen phosphate solution and the pH of the solution was adjusted to ~ 9 by adding NH_4OH. Subsequently, the resultant solution was kept at room temperature under stirring condition for 4 h. Then, the white precipitated was washed with deionized water and followed by the precipitated was spray dried at 200° C with aspiration rate 50 m^3/h. Afterwards, the obtained powder was calcined at 700° C for 3 h. The synthesized HA was characterized by powder X-ray diffraction (XRD) study. The morphology of HA and their particle size distribution was determined by field emission scanning electron microscope (FESEM) and laser diffraction particle size analyser respectively. $DyCl_3$ solution was used as carrier for some radiolabeling studies and prepared by dissolving natural Dy_2O_3 powder in 0.1 M HCl by gentle heating.

The yield of ^{166}Dy and ^{166}Ho produced in equilibrium mixture was determined using High-purity germanium (HPGe) detector (EGG Ortec/Canberra detector, Oak Ridge, Tennessee, USA) coupled with a 4 K multichannel analyser (MCA). The standard ^{152}Eu and ^{133}Ba reference sources were obtained from Amersham Inc., Piscataway, New Jersey, USA. All other radioactivity measurements were performed using a well type NaI(Tl) scintillation detector (Mucha, Elysia-Raytest, Straubenhardt, Germany). Whatman 3 MM chromatography paper (Whatman, Maidstone, Kent, UK) was used for paper chromatography studies. Wistar rats used for biological evaluation of ^{166}Dy/^{166}Ho-labeled HA formulation was bred and reared in the institutional animal house facility of Bhabha Atomic Research Centre. SPECT/CT images were acquired using GE Discovery NM/CT 670 scanner, USA. All animal experiments were carried out following relevant guidelines and regulations approved by the institutional Animal Ethics Committee of Bhabha Atomic Research Centre (Reference: BAEC/12/2024). All experimental methods followed were in accordance with the relevant guidelines and regulations. It is also confirmed that all methods related to animal experiments were performed in accordance with ARRIVE relevant guidelines (https://arriveguidelines.org).

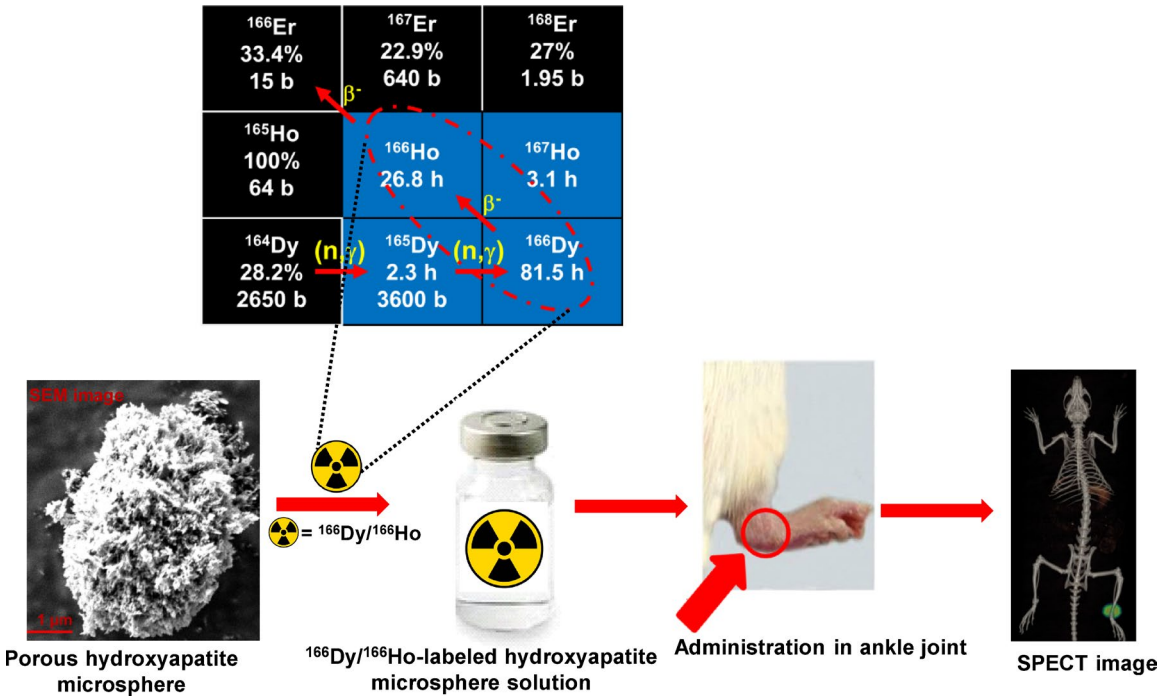

Fig. 1. Schematic representation of production of ^{166}Dy/^{166}Ho, its chelator free radiolabeling with porous hydroxyapatite and pre-clinical evaluation of the radiolabeled formulation for its potential use in RSV.

Production of ^{166}Dy/^{166}Ho

Equilibrium mixture of ^{166}Dy and ^{166}Ho was produced by thermal neutron irradiation of natural Dy_2O_3. Natural Dy consists of seven different isotopes, namely; ^{156}Dy (0.06%), ^{158}Dy (0.10%), ^{160}Dy (2.34%), ^{161}Dy (18.9%), ^{162}Dy (25.5%), ^{163}Dy (24.9%) and ^{164}Dy (28.2%). When natural Dy is irradiated in nuclear reactor, successive thermal neutron captures of ^{164}Dy produces ^{166}Dy and the radionuclide remains in transient equilibrium with the daughter product ^{166}Ho formed by its β^- decay. A weighed amount, typically ~20 mg of natural Dy_2O_3 powder was taken and sealed in a quartz ampoule and subsequently placed inside a standard aluminium irradiation container which was irradiated at a flux thermal neutron flux of ~1.2×10^{14} n/cm^2/s for 14 d at Dhruva reactor, India. After the irradiation, the target was allowed to cool for a period of 24 h to decay the short lived radionuclidic impurities. It was subsequently dissolved in 0.1 M HCl solution by gently heating inside a lead-shielded glove box. The resultant solution was evaporated to near dryness and reconstituted in ~5 mL of deionized water. A measured aliquot of radiochemically processed solution was withdrawn in a glass vial and radioactivity of different radioisotopes present in it was measured using HPGe detector coupled to 4 K MCA system. Energy and efficiency calibration of the detector was carried out using standard ^{152}Eu and ^{133}Ba reference sources before radioactivity measurement and the dead time of the detector during the measurement was ensured to be >2% by appropriate dilution of the sample. The radiochemical purity of ^{166}Dy/^{166}Ho as tri positive metal ions in aqueous solution was ascertained by paper chromatography developed in 0.1 M citrate buffer (pH 4.5) medium[30].

Sorption properties of dy on porous HA

The sorption capacity of porous HA for Dy was calculated by batch equilibration method[1,31] For this, 5 mg of porous HA was equilibrated with 5 mL of $DyCl_3$ solution having different concentration of Dy (0.125–1 mg/mL) at pH ~5.5 and spiked with ~15 µCi (555 kBq) of ^{166}Dy in equilibrium with ^{166}Ho. A reference solution was prepared by taking exactly same amount of ^{166}Dy radioactivity in 5 mL deionized water. The solutions were incubated at room temperature for 1 h. Subsequently, the solutions were centrifuged at 5000 rpm for 10 min and measured aliquot of the supernatants were withdrawn to determine the activity (A_e) using NaI(Tl) detector. An aliquot of same volume was withdrawn from the reference solution and the activity (A_o) was measured using the same NaI(Tl) detector. All measurements were carried out in triplicate. The sorption capacity of porous HA was determined using the following formula:

$$Capacity(q_e) = \frac{(A_o - A_e)V.C_o}{A_o m} \quad (1)$$

where, C_o (mg/mL) was concentration of Dy before sorption, V (mL) was the total volume of solution and m (g) was the mass of porous HA. In order to obtain the rate of transfer of Dy on the surface of porous HA, sorption capacity of porous HA was determined at various time interval for a fixed concentration of Dy (0.5 mg/mL) spiked with ~15 µCi (555 kBq) of ^{166}Dy/^{166}Ho activity.

Determination of optimal conditions for formulation ^{166}Dy/^{166}Ho-labeled porous HA

In order to achieve the maximum radiolabeling yield of formulation of ^{166}Dy/^{166}Ho-labeled porous HA using clinically relevant dose [~ 5 mCi (185 MBq) activity of ^{166}Ho in each dose], the parameters involved in the radiolabeling process were optimized. For this, first radiolabeling was carried out with different concentration (1–10 mg/mL) of porous HA. Weighed amounts (1–10 mg) of porous HA were suspended in deionized water in reaction tubes where ~ 5 mCi (185 MBq) activity of ^{166}Dy/^{166}Ho was added. The pH of the solutions was adjusted to ~ 5–6 and incubated for 1 h at room temperature maintaining the total volume of each reaction mixture 1 mL. A reference solution was prepared by taking exactly same amount of ^{166}Dy radioactivity in 1 mL of deionized water. The reaction mixtures were subsequently centrifuged at 5000 rpm for 10 min. Measured aliquots were withdrawn from each of the reaction mixtures and radioactivity measured (A_s). An aliquot of same volume was withdrawn from the reference and the radioactivity (A_r) was measured. The radiolabeling yield was determined using the following equation:

$$\%Radiolabeling\ yield = (1 - \frac{A_s}{A_r}) \times 100 \tag{2}$$

Additionally, the radiolabeling yield was determined using a standalone method as reported by our group earlier[5] Briefly, the ^{166}Dy/^{166}Ho-labeled porous HA mixture was vortexed thoroughly and centrifuged at 5000 rpm for 10 min after the completion of the reaction. Then, half the volume of the supernatant solution was carefully withdrawn into a test tube and the associated activity was measured using NaI(Tl) detector. In a similar manner, activity associated with HA pellets along with the remaining half of the supernatant solution was also measured using the same NaI(Tl) detector. From these data the percentage radiolabeling yield was determined.

In a similar manner, the radiolabeling yields were determined at various pH (3–7) of the reaction mixture using previous optimized concentration of porous HA. Once the HA concentration and pH were optimized, radiolabeling yields were determined after incubating the reaction mixture at room temperature for different time period to ascertain the optimum incubation time for radiolabeling.

Dose formulation and quality control

Radiolabeling of porous HA was carried out using ~ 5 mCi (185 MBq) of ^{166}Ho in ^{166}Dy/^{166}Ho equilibrium mixture following the following the optimized protocol established from the experiments carried out as discussed in the previous section. The supernatant of the radiolabeled formulation was carefully removed after centrifugation and the pellet of the radiolabeled microparticles was washed with deionized water by repeated vortexing and centrifugation to remove free or loosely bound radioactivity, if present in the formulation. Finally, radiolabeled microparticles were suspended in 1 mL of sterile physiological saline and autoclaved.

The formulation was the subjected to standard quality control tests namely, determination of radionuclidic purity, radiochemical purity, sterility and bacterial endotoxin test (BET). Radionuclidic purity was determined by gamma ray spectrometry using HPGe detector-MCA system by measuring an aliquot of the formulation after thorough mixing. Radiochemical purity was determined following the process described in Sect. 2.4 for determination of radiolabeling yields during optimization studies. The sterility of the ^{166}Dy/^{166}Ho-HA microsphere formulation was assessed using the direct inoculation method, following the approved guidelines in the Indian Pharmacopoeia (IP) using 'Fluid Thioglycolate' and 'Soybean–Casein Digest' media. For this, the test solution was incubated with a portion of the media at the specified temperature (as per IP) for a duration of 14 days. No visible microbial growth in the media ensures the sterility of the formulation. The Gel-Clot-BET assay was conducted to determine apyrogenicity in ^{166}Dy/^{166}Ho-HA microsphere formulation. This method is relied on the coagulation properties of limulus amoebocyte lysate (LAL) which will respond if any endotoxins present in the sample.

In vitro stability assay

Doses of ^{166}Dy/^{166}Ho-HA formulation was prepared as described in Sect. 2.5, centrifuged to separate the supernatant from the labeled particulates. The labeled particulates were then suspended in 1 mL of phosphate buffered saline (PBS, pH ~ 7.4) and incubated at 37° C in a constant temperature incubator. Radiochemical purity for the formulation was determined at regular interval of time upto 14 days from the day of formulation using the procedure already described. Similarly, in vitro stability was determined in freshly isolated human serum at 37° C following the same protocol used for PBS.

Biological studies

Biological evaluation of ^{166}Dy/^{166}Ho-labeled porous HA formulation was carried out by SPECT/CT imaging and ex vivo biodistribution studies in healthy Wistar rats. In vivo stability and pharmacokinetics behaviour of the formulation were thereby ascertained in a pre-clinical setting. For SPECT imaging, 4 healthy Wistar rats (225–250 g) were taken and ~ 0.5 mCi (18.5 MBq) of freshly prepared ^{166}Dy/^{166}Ho-nanoporus HA formulation in 50 µL volume was administered intra-articularly into one of the ankle joints of each animal. Whole body SPECT/CT images were acquired at 3, 24, 48 and 96 h post-administration of the radiolabeled formulation using GE Discovery NM/CT 670 scanner. Animals were anesthetized by controlled CO_2 inhalation prior to the dose administration and acquisition of SPCET/CT images. For ex vivo biodistribution studies, 16 healthy Wistar rats were administered with 0.2 mCi (7.4 MBq) of the formulation in 50 µL volume into one of the ankle joints. The animals were then randomly divided into 4 groups of each having 4 animals. One group of animals were euthanized at 3, 24, 48 and 96 h post-administration by CO_2 asphyxiation. After that, different organs and ankle joints were carefully removed and the weight associated to them were measured. Then the activity of different

organs and ankle joints were measured using NaI(Tl) detector and the dose associated with each organ and ankle joint was expressed in terms of percentage of injected radioactivity dose per organ/tissue.

It is worth mentioning that when freshly prepared ^{166}Dy/^{166}Ho-nanoporus HA formulation is administered into the joint cavity, there could be possibility that ^{166}Ho produced from the β^- decay of its parent ^{166}Dy comes out the HA matrix in the biological system. In such case, the system would not function as an in vivo generator. Hence, it is utmost important to prove that ^{166}Ho did not leach out from the HA matrix and exists in equilibrium with ^{166}Dy after intra-articular administration of the formulation into the joint cavity. For this, γ-spectra were recorded using the injected ankle of ankle joints as the sample after their dissection from the sacrificed Wistar rats at different time intervals post-administration of ^{166}Dy/^{166}Ho-nanoporus HA formulation. Activity of ^{166}Ho was determined using the photo peak at 1379.4 keV for each time point and the decay half-life of ^{166}Ho was determined from this data.

Results and discussion

Characterization of porous HA

The synthesis of porous HA was ascertained by XRD where the peaks appeared in the XRD spectra (Fig. 2A) matches well with the characteristic peaks of hydroxyapatite. The quasi-spherical shape of the microparticles was confirmed by FESEM image (Fig. 2B). The particle size distribution was shown in Fig. 2C which demonstrated that most of the particle used in the study were quasi-spherical in shape with the diameter in the range of 2–10 µm. The porous nature of the synthesized hydroxyapatite was ascertained by N_2 adsorption desorption isotherm study where average pore diameter of the microparticles were found to be ~1.5 nm which make the microparticles porous. The surface area of the porous hydroxyapatite was determined to be ~184 $m^2\ g^{-1}$.

Production of ^{166}Dy/^{166}Ho

Equilibrium mixture of ^{166}Dy/^{166}Ho was produced by successive neutron capture of ^{164}Dy when natural Dy_2O_3 target was irradiated for 14 d at a thermal neutron flux of 1.2×10^{14} n/cm^2/s in Dhruva research reactor at Bhabha Atomic Research Centre. A schematic representation of all the thermal neutron induced nuclear reactions during irradiation of ^{164}Dy is given in Fig. 3. The yields of ^{166}Dy and ^{166}Ho in different batches at the end of irradiation of the target determined by analysis of gamma ray spectra is given in Table 1. It is found that the yield of ^{166}Ho in equilibrium with ^{166}Dy was 17.4 ± 1.2 mCi/mg (643.8 ± 44.4 MBq/mg) of Dy target irradiated. Theoretical yields of ^{166}Ho as a function of irradiation time when 1 mg of natural Dy_2O_3 target is irradiated at a thermal neutron flux of 1.2×10^{14} n/cm^2/s shown Fig. 4. It could be seen that the theoretical yield of ^{166}Ho is close

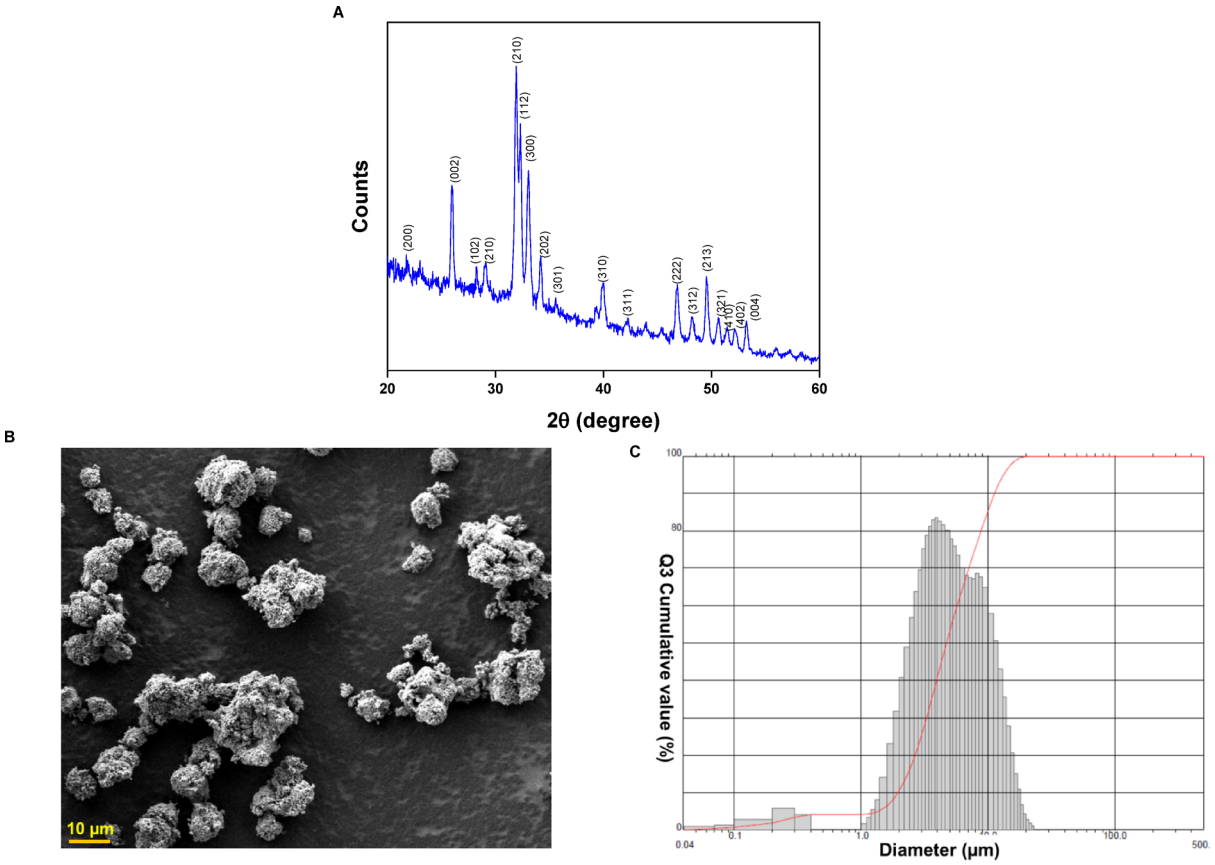

Fig. 2. XRD pattern (**A**), FESEM image (**B**) and particle size distribution (**C**) of porous HA microsphere.

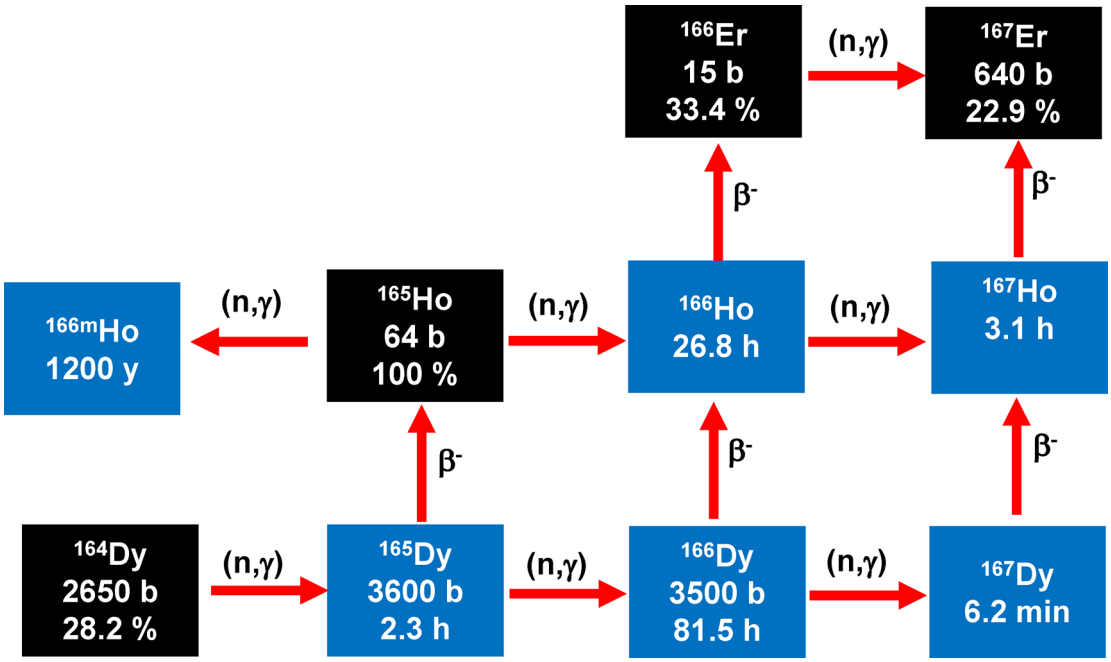

Fig. 3. Schematic representation of the major thermal neutron induced nuclear reactions during irradiation of ^{164}Dy in nuclear reactor.

Batch No	Amount of Dy_2O_3 irradiated (mg)	Duration of irradiation (d)	Production yield mCi (GBq)	
			^{166}Dy	^{166}Ho
1	22.9	14	295 (10.9)	346 (12.8)
2	22.8	14	287 (10.6)	338 (12.5)
3	23.1	14	302 (11.2)	354 (13.1)
4	23.4	14	308 (11.4)	360 (13.3)

Table 1. Yields of ^{166}Dy and ^{166}Ho produced by irradiation of natural Dy_2O_3 targets in Dhruva reactor at a thermal flux of 1.2×10^{14} N cm^{-2} s^{-1} in different batches.

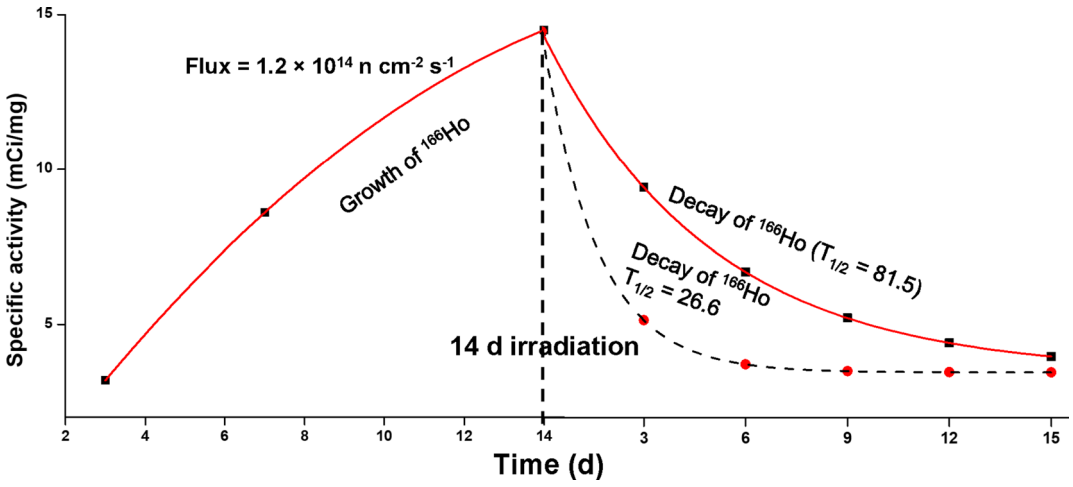

Fig. 4. Growth and decay of ^{166}Ho produced from successive neutron capture of ^{164}Dy when irradiated at a thermal neutron flux of 1.2×10^{14} n/cm^2/s based on theoretical calculations.

to that of practically obtained value for 14 d irradiation. Since ^{166}Ho produced in this route exists in transient equilibrium with ^{166}Dy, the activity of ^{166}Ho will decay following the half-life of ^{166}Dy ($T_{1/2}$ = 81.5 h) after the end of irradiation. This is depicted by the solid line in Fig. 4, while black dotted line shows the decay of ^{166}Ho by its own half-life ($T_{1/2}$ = 26.8 h). Therefore, when ^{166}Dy/^{166}Ho couple acts as in vivo generator of ^{166}Ho, the cumulative radiation dose delivered becomes significantly higher compared to that from the same activity ^{166}Ho alone[32] This clearly demonstrates the advantage of production of ^{166}Ho from neutron irradiation Dy_2O_3 target.

Assay of radionuclidic impurities co-produced with ^{166}Dy/^{166}Ho, if any, was carried out from the γ- ray spectra. A typical gamma ray spectrum recorded 24 h after radiochemical processing of neutron irradiated Dy_2O_3 target (Fig. 5A) shows only the photopeaks correspond to those of ^{166}Dy and ^{166}Ho. The radiochemical purity of ^{166}Dy/^{166}Ho was ascertained by paper chromatography (Fig. 5B) developed in 0.1 M citrate buffer (pH ~4.5) and it was observed that the free [^{166}Dy/^{166}Ho]Dy^{3+} ion moved in the solvent front (R_f= 0.8–1) while colloidal particles remained at the point of application (R_f= 0–0.1). This study indicated that >99% of ^{166}Dy/^{166}Ho exist in the form of [^{166}Dy/^{166}Ho]$DyCl_3$ which is suitable for the radiolabeling with porous HA.

Sorption properties of dy on porous HA

The sorption capacity (q_e, mg/g) of porous HA for the Dy was determined at different concentration of Dy and it was shown in the **Figure S1**. It is evident that sorption capacity initially increases with increased in concentration of Dy and then reached state of saturation. The maximum sorption capacity of porous HA for the Dy was found to be 272 ± 12 mg/g. Subsequently, equilibrium concentration (C_e, mg/L) of Dy was calculated from the experimental data of percentage of sorption of Dy on porous HA. The variation of q_e as function of C_e was determined and linearly fitted them with the various sorption isotherm (**Table S1**) by converting them into appropriate algebraic form. It was observed that sorption of Dy on the surface of porous HA followed Langmuir-Freundlich (L-F) isotherm (Fig. 6A) and Langmuir isotherm (**Figure S2 A)** and Freundlich isotherm (**Figure S2B**) could be ruled out due to poor correlation coefficient values.

Kinetics of the sorption of Dy on porous HA was established by measuring sorption capacity as a function of time and it was observed that sorption capacity increases with increasing the incubation time (**Figure S3 A**) and reached state of saturation. The rate of sorption was determined by plotting sorption capacity against time after converting them into suitable algebraic form and linearly fitted them into two types of kinetic model (**Table S1**). It was found that sorption of Dy on porous HA followed pseudo-second order kinetics (Fig. 6B) and the rate constant of the sorption was found to be 1.82×10^{-3} $g.mg^{-1}.min^{-1}$. The pseudo-first order model (**Figure S3B)** was discarded due to its poor correlation coefficient value. Adherence to L-F isotherm as well as pseudo-second order kinetics indicates chemisorption of Dy on the surface of porous HA matrix[33] This chemical interaction would ensure the robust in vitro and in vivo stability of the radiolabeled formulation.

The superiority of the synthesized porous HA microsphere over the commercially available bulk HA was demonstrated by comparing the sorption capacity of these matrix for ^{166}Dy. The results were summarized in **Table S2**. It is shown that the porous HA exhibited ~2.7 times higher sorption capacity compared to bulk HA. This is attributed to high surface area of porous HA compared to bulk HA. The high sorption capacity is especially relevant for the preparation of radiolabeled formulation using low specific activity radiometals such as ^{166}Dy produced from double neutron capture of ^{164}Dy. Moreover, the high sorption capacity can prolong the shelf-life of the radiolabeled HA which can be transported to distant user site.

Determination of optimal conditions for formulation ^{166}Dy/^{166}Ho-labeled porous HA

The radiolabeling yields of ^{166}Dy/^{166}Ho-nanopours HA were evaluated using ~5 mCi (185 MBq) ^{166}Ho activity (in equilibrium with ^{166}Dy) at different concentration of porous HA while keeping the pH of the solution ~5–6. The radiolabeling yield was determined by employing both the methods as described in the experimental

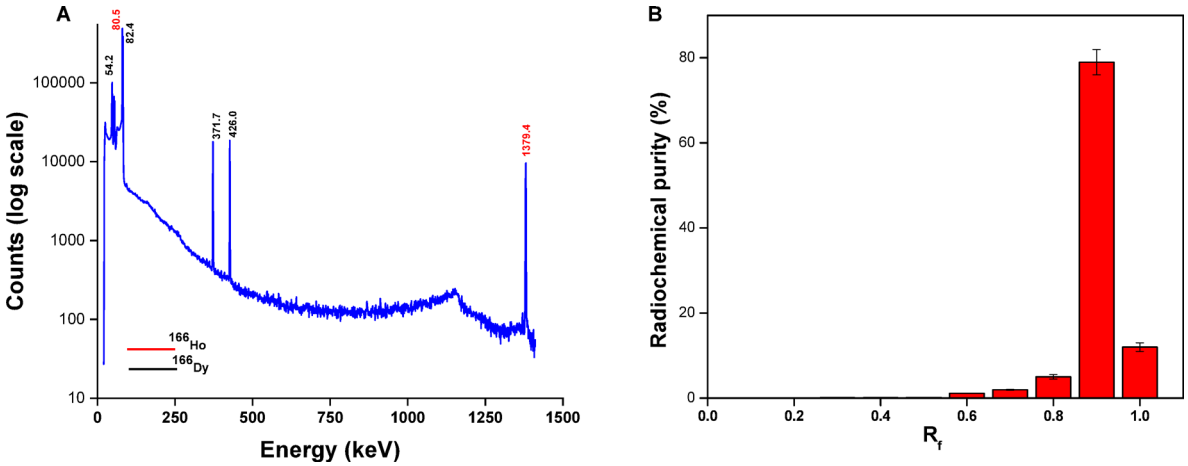

Fig. 5. (**A**) Typical γ-ray spectrum of ^{166}Dy/^{166}Ho recorded 24 h after radiochemical processing of neutron irradiated Dy_2O_3 target and (**B**) paper chromatography pattern of chemically processed [^{166}Dy/^{166}Ho]$DyCl_3$ solution developed in 0.1 M citrate buffer (pH ~4.5).

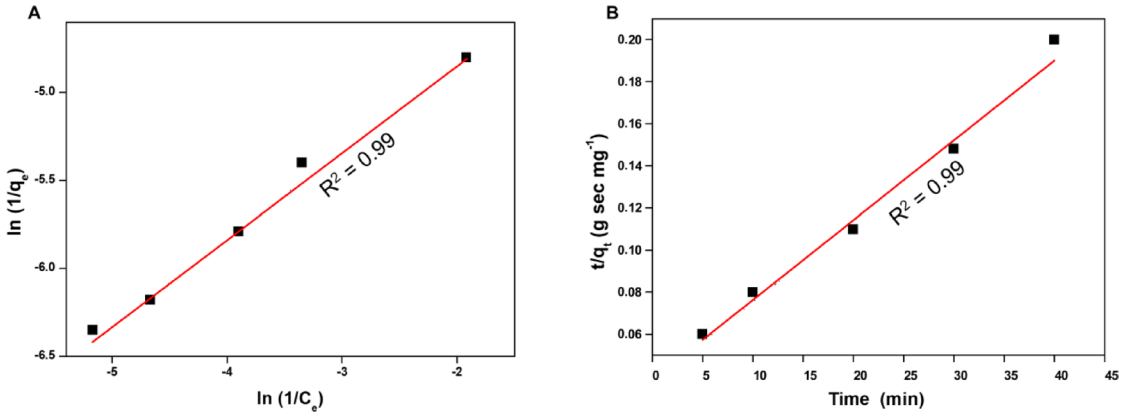

Fig. 6. Linear fitting of (**A**) Langmuir-Freundlich isotherm model and (**B**) pseudo-second order kinetics for sorption of ^{166}Dy/^{166}Ho ion on porous HA at room temperature.

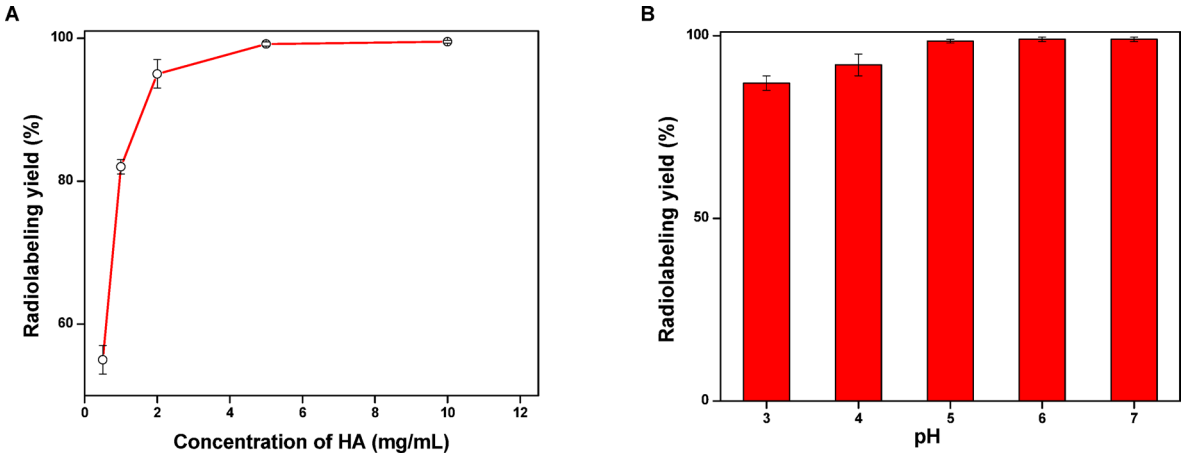

Fig. 7. Variation of radiolabeling yield of ^{166}Dy/^{166}Ho-nanoporous HA microsphere at (**A**) different concentration of HA at a fixed pH of ~ 5–6 and (**B**) different pH of the solution using 5 mg/mL concentration of HA.

section and it was observed that both the methods give comparable results. It was found that the radiolabeling yield increased with increasing the concentration of porous HA and beyond a concentration (5 mg/mL) state of saturation was achieved (Fig. 7A). Subsequently, the radiolabeling yield was evaluated at various pH of the solution while keeping the concentration of porous HA fixed at 5 mg/mL. It was observed that the radiolabeling yield reached at saturation state at pH ~ 5 (Fig. 7B) and beyond pH ~ 6, radiolabeling of porous HA with ^{166}Dy/^{166}Ho was not recommended due to precipitation of radiolanthanides in the form of their hydroxide. Further, radiolabeling studies using 5 mg/mL of nonporous HA at pH ~ 5 for different duration of incubation at room temperature showed that at 30 min incubation the radiolabeling yield reached > 97%. The optimized radiolabeling protocol yielding > 97% radiolabeling yield is schematically presented in Fig. 8.

Several doses of ^{166}Dy/^{166}Ho-labeled porous HA were formulated using the optimized protocol and quality parameters as mentioned in Sect. 2.5 were checked. The results were summarized in Table 2. It could be seen that, in all the cases sterile and pyrogen free doses of the formulation were obtained with > 99.9% radionuclidic purity and > 98.0% radiochemical purity.

In vitro stability of ^{166}Dy/^{166}Ho-porous HA formulation

In vitro stability of ^{166}Dy/^{166}Ho-porous HA formulation prepared under optimized conditions was investigated in PBS and human serum. It was found that even after 14 days, the radiolabeled formulation maintained its radiochemical integrity > 98% in both the cases (Fig. 9). Also, during the investigation of radiochemical stability of ^{166}Dy/^{166}Ho-porous HA in human serum, aliquot from the supernatant was withdrawn and γ-ray spectra were recorded (**Figure S4**). It did not show photopeaks corresponding to ^{166}Ho. This indicated that there was practically no leaching of ^{166}Ho from matrix of porous HA. This in vitro study suggested minimal degradation or loss of radiolabeled formulation under physiological conditions.

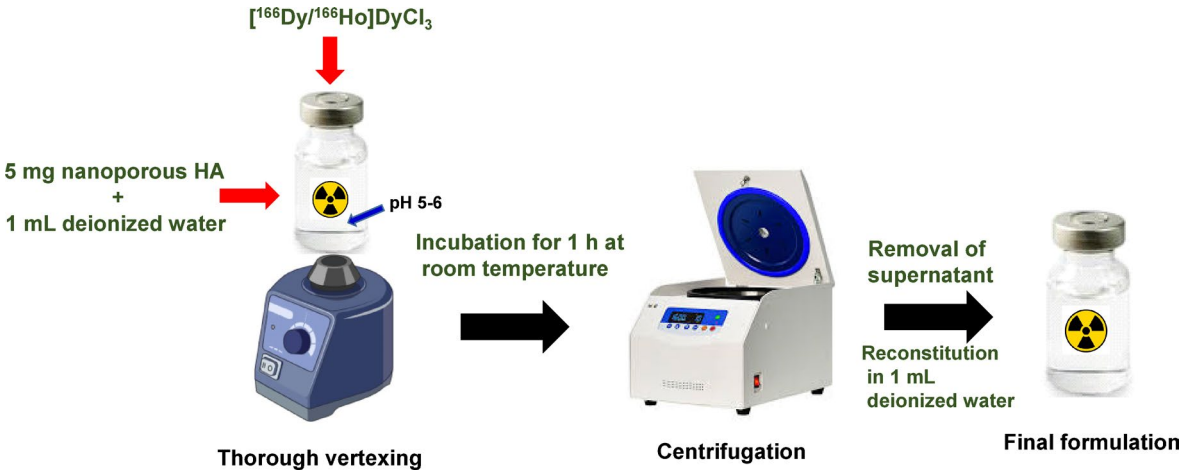

Fig. 8. Schematic representation for the optimized protocol for formulation of a dose of ^{166}Dy/^{166}Ho-labeled porous HA microsphere.

Batch No	Concentration of porous HA (mg/mL)	Amount of ^{166}Ho (in equilibrium with ^{166}Dy) activity added mCi (MBq)	Formulation yield (%)	Radionuclidic purity (%)	Radiochemical purity (%)
1	5	5.2 (192.4)	97.5 ± 1.2	> 99.9 ± 0.01%	98.8 ± 1.2
2	5	5.6 (207.2)	98.2 ± 0.8	> 99.9 ± 0.03%	99.1 ± 0.5
3	5	5.5 (203.5)	97.8 ± 1.1	> 99.9 ± 0.02%	98.7 ± 1.1
4	5	5.0 (185)	98.7 ± 0.5	> 99.9 ± 0.01%	99.5 ± 0.6
5	5	5.5 (203.5)	97.9 ± 0.9	> 99.9 ± 0.02%	99.2 ± 0.3

Table 2. Batch wise yield of ^{166}Dy/^{166}Ho-HA formulation for preclinical study.

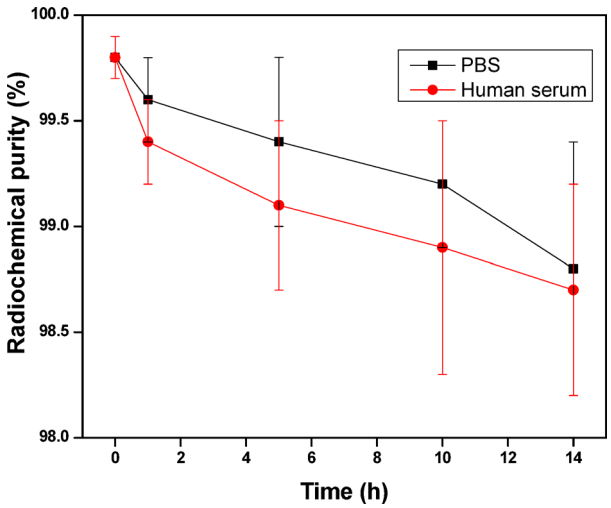

Fig. 9. In vitro stability of ^{166}Dy/^{166}Ho-porous HA in PBS and human serum.

Biological study

The localization of ^{166}Dy/^{166}Ho-porous HA in the synovial joint and its in vivo stability was investigated by acquiring SPECT/CT images at different time point after the intra-articular administration of the radiolabeled formulation in the ankle joint. The images (Fig. 10A) showed that the administered ^{166}Dy/^{166}Ho-porous HA microsphere formulation was completely retained within the ankle joint cavity even after 96 h of post administration and during this time period there was no translocation of the ^{166}Dy/^{166}Ho radionuclide *in vivo*. These observations were corroborated by ex vivo biodstribution studies. The results of biodistribution studies (Fig. 10B) were also demonstrated near-complete retention of ^{166}Dy/^{166}Ho-porous HA microsphere after 96 h

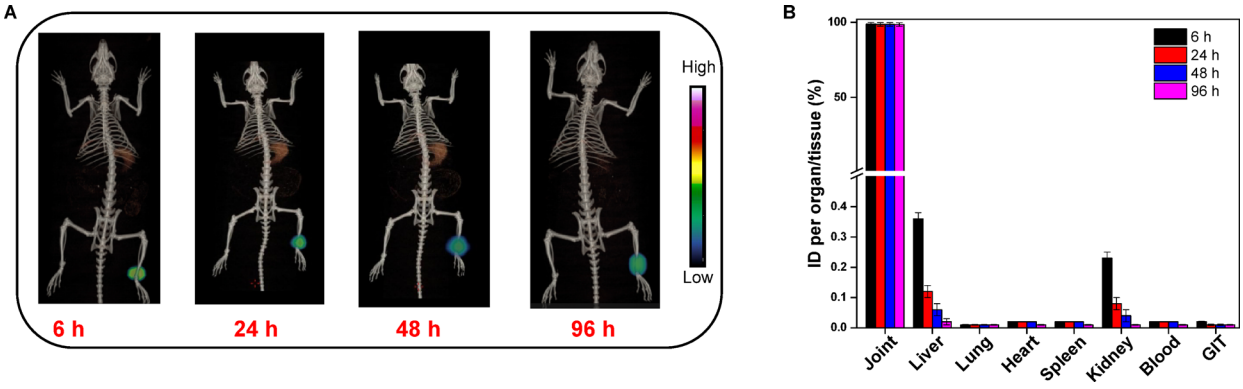

Fig. 10. (**A**) SPECT/CT images of healthy Wistar rat injected with the ^{166}Dy/^{166}Ho-porous HA microsphere in one of the knee joints at various time points of post injection and (**B**) results of ex vivo biodistribution study.

Organ/Tissue	ID per organ/tissue (%)		
	^{169}Er-HA	^{188}Re-HA	^{166}Dy/^{166}Ho-porous HA
Blood	0.01 ± 0.01	0.06 ± 0.02	0.02 ± 0.01
Liver	0.23 ± 0.04	0.03 ± 0.01	0.12 ± 0.02
GIT	0.04 ± 0.02	0.36 ± 0.12	0.01 ± 0.002
Kidney	0.00 ± 0.00	0.02 ± 0.01	0.08 ± 0.02
Spleen	0.02 ± 0.01	0.003 ± 0.003	0.02 ± 0.001
Lungs	0.02 ± 0.01	0.012 ± 0.003	0.01 ± 0.001
Injected Joint	98.22 ± 1.28	97.45 ± 0.40	98.62 ± 1.21

Table 3. Comparison of ex vivo biodistribution pattern of ^{166}Dy/^{166}Ho-porous HA microsphere with ^{169}Er-HA and ^{188}Re-HA at 48 h post injection.

of post administration of the formulation. There was almost no uptake of the formulation in any of the organ/tissue. The ex vivo biodistribution pattern of ^{166}Dy/^{166}Ho-porous HA microsphere formulation was compared with two other radiolabeled hydroxyapatite microparticles namely, ^{169}Er- and ^{188}Re-labeled HA microparticles, reported in the literature (Table 3)[34,35] The data shows comparable biodistribution pattern of ^{166}Dy/^{166}Ho-porous HA microparticles with the formulations mentioned.

In order to establish the potential utility ^{166}Dy/^{166}Ho-porous HA formulation as an in vivo generator of ^{166}Ho, the ankle joints dissected from the animals at different time points post-injection were analyzed by γ-ray spectrometry and ^{166}Ho activity determined. Subsequently, the decay half-life of ^{166}Ho was calculated by plotting the ^{166}Ho activity in the joints of the animals sacrificed at different time points post-injection and found to be 83.4 h, which is very close to the half-life of ^{166}Dy ($T_{1/2}$ = 81.5 h). Therefore, this study precludes the release of ^{166}Ho from HA matrix demonstrates that the formulation functions as an in vivo generator of ^{166}Ho. A typical γ-ray spectrum of the injected ankle joint of an animal and variation ^{166}Ho activity in the joints of the animals sacrificed at different time points post-injection are shown in Figs. 11**(A)** and **(B)**, respectively.

Conclusion

In summary, we report the production of ^{166}Ho from indirect route by thermal neutron bombardment on natural Dy_2O_3 as target in nuclear reactor and optimized the chelator-free radiolabeling protocol for formulation of ^{166}Dy/^{166}Ho-labeled porous HA, where ^{166}Ho exists in transient equilibrium with ^{166}Dy. The remarkable in vitro stability of the radiolabled porous HA microsphere was demonstrated in PBS and human serum at physiological temperature over a period of 14 days. The Biological study showed complete retention of the injected ^{166}Dy/^{166}Ho-porous HA in the synovial cavity without any translocation of parent or daughter radioisotope in vivo and thus exhibiting its potential use as in vivo generator. Overall, this in vivo generator strategy would pave a new avenue towards effective management of chronic inflammatory joint diseases.

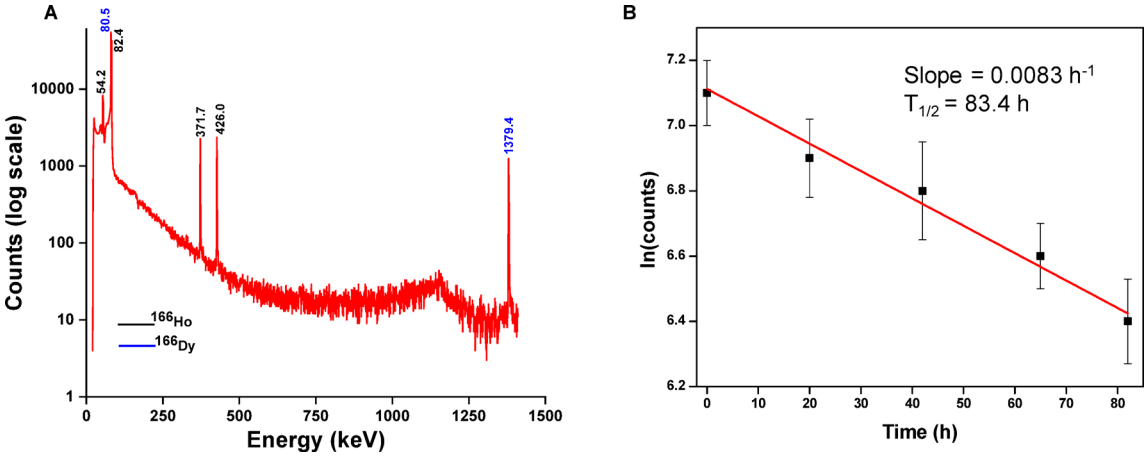

Fig. 11. (**A**) A typical γ-ray spectrum of the injected ankle joint of a healthy Wistar rat and (**B**) variation ^{166}Ho activity in the joints of the animals sacrificed at different time points post-injection.

Data availability

All the data used and/or analysed during the current study are available from the corresponding author on reasonable request.

Received: 31 January 2025; Accepted: 13 May 2025
Published online: 20 May 2025

References

1. Patra, S. et al. Radiolabeled porous hydroxyapatite microspheres: an advanced material for potential use in radiation synovectomy. *Mater. Chem. Phys.* **295**, 127115. https://doi.org/10.1016/j.matchemphys.2022.127115 (2023).
2. Vimalnath, K. V., Rajeswari, A., Patra, S., Kamaleshwaran, K. K. & Chakraborty, S. Multi-dose formulation and clinical deployment of [^{90}Y] Y-labeled hydroxyapatite (HA) microparticles for radiation synovectomy in India–the inherent intricacies. *Appl. Radiat. Isot.* **111644** https://doi.org/10.1016/j.apradiso.2024.111644 (2025).
3. Zayeni, H. et al. The effect of radiation synovectomy with phosphorus-32 on the pain and swelling in 31 RA patients with resistant monoarthritis of the knee. *Clin. Rheumatol.* **43**, 2791–2798. https://doi.org/10.1007/s10067-024-07058-4 (2024).
4. Guldem, M., Goksel, A., Yusuf, O. & Cermik, T. Formulation and in-vivo characterization of ^{177}Lu-tin-colloid as a radiosynovectomy agent. *Curr. Radiopharm.* **17** (9), 68–76. https://doi.org/10.2174/0118744710252994231024064842 (2024).
5. Chakraborty, S., Das, T., Banerjee, S., Sarma, H. D. & Venkatesh, M. Preparation and preliminary biological evaluation of ^{177}Lu-labelled hydroxyapatite as a promising agent for radiation synovectomy of small joints. *Nucl. Med. Commun.* **27** (8), 661–668. https://doi.org/10.1097/00006231-200608000-00008 (2006).
6. Deutsch, E., Brodack, J. W. & Deutsch, K. F. Radiation synovectomy revisited. *Eur. J. Nucl. Med.* **20**, 1113. https://doi.org/10.1007/BF00173494 (1993).
7. Ahmad, I. & Nisar, H. Dosimetry perspectives in radiation synovectomy. *Phys. Med.* **47**, 64–72. https://doi.org/10.1016/j.ejmp.2018.02.015 (2018).
8. dos Santos, M. F. et al. Effectiveness of radiation synovectomy with samarium-153 particulate hydroxyapatite in rheumatoid arthritis patients with knee synovitis: a controlled randomized double-blind trial. *Clinics* **64**, 1187. https://doi.org/10.1590/S1807-59322009001200008 (2009).
9. Kampen, W. U. et al. Long-term results of radiation synovectomy: a clinical fellow-up study. *Nucl. Med. Commun.* **2**, 239–246. https://doi.org/10.1097/00006231-200102000-00017 (2001).
10. Zuckerman, J. D., Sledge, C. B., Shortkroff, S. & Venkateshan, P. Treatment of rheumatoid arthritis using radiopharmaceuticals. *Nucl. Med. Biol.* **14**, 211–218. https://doi.org/10.1016/0883-2897(87)90044-4 (1987).
11. Sledge, C. B., Noble, J., Hnatowich, D. J., Kramer, R. & Shortkroff, S. Experimental radiation synovectomy by ^{165}Dy ferric hydroxide macroaggregates. *Arthritis Rheum.* **20**, 1334–1342. https://doi.org/10.1002/art.1780200706 (1997).
12. Pandey, U. et al. Evaluation of ^{90}Y phosphate particles as a possible radiation synoviorthesis agent. *Nucl. Med. Commun.* **26**, 459–463. https://doi.org/10.1097/00006231-200505000-00011 (2005).
13. Rajeswari, A. et al. Hydroxyapatite (HA) microparticles labeled with ^{32}P – A promising option in the radiation synovectomy for inflamed joints. *Appl. Radiat. Isot.* **116**, 85–91. https://doi.org/10.1016/j.apradiso.2016.07.022 (2016).
14. Rizaludin, A. et al. Phosphorus–32 labelled irradiated bovine hydroxyapatite for radiosynovectomy. *J. Radioanal Nucl. Chem.* https://doi.org/10.1007/s10967-024-09917-5 (2024).
15. Santos, A. O. et al. Knee radiosynovectomy with ^{153}Sm-hydroxyapatite compared to ^{90}Y-hydroxyapatite: initial results of a prospective trial. *Ann. Nucl. Med.* **35**, 232–240. https://doi.org/10.1007/s12149-020-01557-5 (2021).
16. Chakraborty, S. et al. Preparation, evaluation, and first clinical use of ^{177}Lu-labeled hydroxyapatite (HA) particles in the treatment of rheumatoid arthritis: utility of cold kits for convenient dose formulation at hospital radiopharmacy. *J. Label. Compd. Radiopharm.* **57**, 453–462. https://doi.org/10.1002/jlcr.3202 (2014).
17. Shinto, A. S. et al. Radiosynovectomy of painful synovitis of knee joints due to rheumatoid arthritis by intra–articular administration of ^{177}Lu–labeled hydroxyapatite particulates: first human study and initial Indian experience. *World J. Nucl. Med.* **14**, 81–88. https://doi.org/10.4103/1450-1147.153908 (2015).
18. Vimalnath, K. V. et al. Radiochemistry, pre-clinical studies and first clinical investigation of ^{90}Y-labeled hydroxyapatite (HA) particles prepared utilizing ^{90}Y produced by (n,γ) route. *Nucl. Med. Biol.* **42**, 455–464. https://doi.org/10.1016/j.nucmedbio.2015.01.006 (2015).
19. Nazar, A. K. & Basu, S. A. Multidimensional overview of diagnostic and therapeutic nuclear medicine: current status and the evolving concepts. In *Handbook on Radiation Environment* Vol. 1 (ed. Aswal, D. K.) (Springer, 2024). https://doi.org/10.1007/978-981-97-2795-7_8.

20. Ofluoglu, S. et al. Radiation synovectomy with ^{166}Ho-ferric hydroxide: a first experience. *J. Nucl. Med.* **43**, 1489–1494 (2002).
21. Unni, P. R., Chaudhari, P. R., Venkatesh, M., Ramamoorthy, N., Pillai, M. R. A. & N. & Preparation and bioevaluation of ^{166}Ho labeled hydroxyapatite (HA) particles for radiosynovectomy. *Nucl. Med. Biol.* **29**, 199–209. https://doi.org/10.1016/s0969-8051(01)00303-1 (2002).
22. Bagheri, R. & Ranjbar, H. Animal-based radiation absorbed dose evaluation of holmium-166 labeled hydroxyapatite particulates in liver malignancies. *Asia Ocean. J. Nucl. Med. Biol.* **13**, 94–101. https://doi.org/10.22038/aojnmb.2024.79679.1560 (2025).
23. Klaassen, N. J. M., Arntz, M. J., Arranja, A. G., Roosen, J. & Nijsen, J. R. The various therapeutic applications of the medical isotope holmium-166: a narrative review. *Radiopharm Chem.* **4**, 19. https://doi.org/10.1186/s41181-019-0066-3 (2019). E.J.N.M.M.I
24. Bahrami, S. A. et al. Production, quality control and Pharmacokinetic studies of ^{166}Ho-EDTMP for therapeutic applications. *Sci. Pharm.* **78**, 423–433. https://doi.org/10.3797/scipharm.1004-21 (2010).
25. Lahiri, S., Volkers, K. J. & Wierczinski, B. Production of ^{166}Ho through ^{164}Dy(n,γ)165Dy(n,γ)^{166}Dy(β^-)^{166}Ho and separation of ^{166}Ho. *Appl. Radiat. Isot.* **61**, 1157–1161. https://doi.org/10.1016/j.apradiso.2004.03.117 (2004).
26. Dadachova, E., Mirzadeh, S., Lambrecht, R. M., Hetherington, E. L. & Knapp, F. F. jr Separation of carrier-free holmium-166 from neutron-irradiated dysprosium targets. *Anal. Chem.* **66**, 4272–4277 (1994).
27. Smith, S. V. et al. [^{166}Dy]Dysprosium/[^{166}Ho]Holmium in vivo generator. *Appl. Radiat. Isot.* **46**, 759–764. https://doi.org/10.1016/0969-8043(94)00149-T (1995).
28. Flores, G. F. et al. [^{166}Dy]Dy/^{166}Ho hydroxide macroaggregates: an in vivo generator system for radiation synovectomy. *Appl. Radiat. Isot.* **61**, 1227–1233. https://doi.org/10.1016/j.apradiso.2004.04.018 (2004).
29. Zeevaart, J. R., Szücs, Z., Takacs, S., Jarvis, N. V. & Jansen, D. Recoil and conversion electron considerations of the ^{166}Dy/^{166}Ho in vivo generator. *Radiochim Acta.* **100**, 109–113. https://doi.org/10.1524/ract.2011.1841 (2012).
30. Chakravarty, R., Patra, S., Jagadeesan, K. C., Thakare, S. V. & Chakraborty, S. Electrochemical separation of $^{132/135}$La theranostic pair from proton irradiated Ba target. *Sep. Purif. Technol.* **280**, 119908. https://doi.org/10.1016/j.seppur.2021.119908 (2022).
31. Patra, S. et al. Chelator-free radiolabeling with theoretical insights and preclinical evaluation of citrate-functionalized hydroxyapatite nanospheres for potential use as radionanomedicine. *Ind. Eng. Chem. Res.* **62**, 3194–3205. https://doi.org/10.1021/acs.iecr.2c04378 (2023).
32. Wang, R., Ponsard, B., Wolterbeek, H. & Denkova, A. Core–shell structured gold nanoparticles as carrier for ^{166}Dy/^{166}Ho in vivo generator. *E J. N M M I Radiopharm Chem.* **7**, 16. https://doi.org/10.1186/s41181-022-00170-3 (2022).
33. Correa, F. G., Granados, J. V., Reyes, M. J. & Granados, L. A. Q. Adsorption behaviour of La(III) and Eu(III) ions from aqueous solutions by hydroxyapatite: kinetic, isotherm, and thermodynamic studies. *J. Chem.* **2013(1)**, 751696. https://doi.org/10.1155/2013/751696 (2013).
34. Chakraborty, S., Das, T., Chirayil, V., Lohar, S. P. & Sarma, H. D. Erbium-169 labeled hydroxyapatite particulates for use in radiation synovectomy of digital joints – a preliminary investigation. *Radiochim Acta*. **102** (5), 443–450. https://doi.org/10.1515/ract-2013-2166 (2014).
35. Kothari, K., Suresh, S., Sarma, H. D., Meera, V. & Pillai, M. R. A. ^{188}Re-labeled hydroxyapatite particles for radiation synovectomy. *Appl. Radiat. Isot.* **58**, 463–468 (2003). 10.1016/S0969-8043(03)00028 – 9.

Acknowledgements

The authors would like to thank Dr. Tapas Das, Head, Radiopharmaceuticals Division, BARC for his support. The authors are also grateful to Dr. Sandip Basu, Head, Radiation Medicine Centre (Medical), BARC, and Shri. N. S. Baghel Head, Radiation Medicine Centre (General), BARC for allowing to use the animal house facility.

Author contributions

S.P. carried out experiments and wrote main manuscriptK.S., A.C., S.K.M. and S.R. carried out experimentsR.C. reviewed the main manuscriptS.C. conceptualized the work and reviewed the main manuscript.

Funding

Open access funding provided by Department of Atomic Energy.

Declarations

Competing interests

The authors declare no competing interests.

Additional information

Supplementary Information The online version contains supplementary material available at https://doi.org/10.1038/s41598-025-02373-5.

Correspondence and requests for materials should be addressed to S.C.

Reprints and permissions information is available at www.nature.com/reprints.

Publisher's note Springer Nature remains neutral with regard to jurisdictional claims in published maps and institutional affiliations.